

Pattern transfer of electron beam modified self-assembled monolayers for high-resolution lithography

M. J. Lercel, M. Rooks, R. C. Tiberio, and H. G. Craighead

School of Engineering and Applied Physics and the National Nanofabrication Facility, Cornell University, Ithaca, New York 14853

C. W. Sheen, A. N. Parikh, and D. L. Allara

Department of Materials Science and Department of Chemistry, Pennsylvania State University, University Park, Pennsylvania 16802

(Received 30 September 1994; accepted 12 December 1994)

Self-assembled monolayers of octadecylsiloxane and octadecylthiol have been modified by high-resolution electron beam lithography. Focused electron beams from 1 to 50 keV and scanning tunneling microscopy at ~ 10 eV have been used as patterning tools. The patterns have been transferred into many substrates by wet, dry, and combinations of wet and dry etches. Wet etching almost always results in a positive tone, but reactive ion etching of GaAs with Cl_2 at very low dc biases (< 10 V) results in a negative tone. The effect of electron beam damage on the monolayers and the subsequent etching reactions has been explored through x-ray photoelectron spectroscopy. © 1995 American Vacuum Society.

I. INTRODUCTION

Future lithography may require nanometer-scale dimensions, and even now there is a strong desire for ≤ 25 nm lithography for research purposes. Thin, high-resolution resists are needed if low-energy lithography tools such as fabricated microcolumns¹ are going to be practical. Self-assembled monolayers (SAMs) are a possible tool for the fabrication of nanometer-scale devices. The molecules in SAMs are very small compared to those in most conventional polymeric resists. SAMs can form high-coverage, durable, thin (< 5 nm) films easily,^{2,3} which is very difficult to do with polymeric resists. There is interest in the use of SAMs for high-resolution patterning, particularly with low-energy electrons that have very short penetration depths. SAMs have been shown to work as electron beam resists for wet chemical pattern transfer at doses less than or comparable to other high-resolution electron beam resists⁴⁻⁶ and also for selective electroless metallization,⁷ electroplating,⁸ selective mineralization,⁹ and selective monolayer deposition.^{10,11}

Self-assembled monolayer based resists have also been explored for scanning tunneling microscopy (STM) lithography. At these very low beam energies, the electron penetration is very short, and thin (~ 2.5 nm) monolayers are an excellent choice for ultra-high-resolution work. STM patterning of organothiols on both Au and GaAs have been reported, and they have been used as resists for wet chemical pattern transfer,¹² selective chemical vapor deposition,¹³ and electrochemical etching.¹⁴ STM patterned organosilanes have been used for selective metal deposition.⁷

In this article, we report studies on electron beam patterning of self-assembled monolayers and subsequent pattern transfer by both wet and dry etching. The interaction of the etches with the SAM surfaces is discussed. For this study, the SAMs of octadecyltrichlorosilane [OTS, $\text{CH}_3(\text{CH}_2)_{17}\text{SiCl}_3$] on silicon dioxide and titanium dioxide and octadecylthiol

[ODT, $\text{CH}_3(\text{CH}_2)_{17}\text{SH}$] on gold and GaAs were prepared as we have reported earlier.⁴⁻⁶

II. ELECTRON BEAM PATTERNING OF SAMs

Self-assembled monolayers were exposed to electron beams from very low (~ 10 eV) to very high (50 keV) energy. A JEOL JBX 5DIIU electron beam lithography system was used to expose patterns at 50 keV and 100 pA beam current with a resolution of ~ 25 nm. An Hitachi S-800 scanning electron microscope with a pattern generator was used for 1–25 keV exposures.

The patterns written into the monolayer were inspected by atomic force microscopy (AFM).^{5,6} This inspection allows separation of the size of the actual beam damage region from the resulting line sizes after pattern transfer (which increase for isotropic etches). A Digital Instruments Nanoscope III was used for both contact and tapping mode (TM) AFM imaging. The exposed regions of the monolayer are visible as small height variations in both AFM modes. However, for contact AFM large frictional changes in the surface were seen as significant changes in apparent height for forward and reverse tip motion.¹⁵

For very low electron energies, a scanning tunneling microscope (also the Nanoscope III) was operated with tip-sample biases up to 10 V (tip negative) to expose layers of ODT on Au and GaAs. The minimum line size from the STM exposures depends very strongly on the tip radius and tip-sample spacing.¹² The minimum line size exposed was ~ 15 nm; however, this was determined by an AFM measurement, and the effect of the AFM tip radius on the measurement is certain to account for some of that width. Typical doses for STM exposures were ~ 30 nC/cm, which is more than a factor of 10 higher than the minimum doses for 50 keV exposures.

III. PATTERN TRANSFER

Previously, we have shown that a variety of wet etches can be used to transfer patterns exposed in a self-assembled monolayer to the underlying substrate.^{4–6} In almost all cases with wet etching, the alkylsiloxanes and alkylthiols act as self-developing positive resists. Even STM exposed layers of ODT on Au and GaAs act as positive resists when etched with KI/I_2 and NH_4OH , respectively.^{6,12} Silicon dioxide and titanium have been patterned using OTS layers and hydrofluoric acid etches, and silicon has been etched with KOH to depths >120 nm.⁶ Certain etches are more favorable for use with monolayer resists. Strong oxidizers, especially hydrogen peroxide, lead to rapid destruction of the SAM resist layer. For example, an ODT layer on GaAs will remain intact for at least 60 min in dilute NH_4OH , but the addition of even a small amount ($\sim 10\%$) of hydrogen peroxide will reduce survival time to less than 2 min.

Although wet etches have been successful for pattern transfer, almost all of them are isotropic, so that it would be advantageous to have a more anisotropic process. However, SAMs make poor etch masks for conventional reactive ion etches (RIE) because they are thin. Therefore, bilayer processes have been explored that should be able to provide for higher etch anisotropy and etch depths. In this process, the patterned monolayer is used as a wet etch mask for a thin oxide or metal layer. Subsequently, the thin oxide or metal layer provides a mask for a reactive ion etch. Thermally grown SiO_2 layers (30 nm thick) patterned with an OTS layer were used as masks for a Cl_2 RIE to etch ~ 80 nm into the silicon substrate.⁶ Similarly, a 15 nm evaporated SiO_2 layer on GaAs was used to etch into the GaAs; however, the poor adhesion of the SiO_2 on the GaAs caused the oxide to float off the GaAs surface during the wet etch.¹⁶

Since these materials are being explored for ultra-high-resolution resists, the processing must also be able to transfer patterns at small dimensions. Since hydrofluoric acid etching of SiO_2 is isotropic, etching through an oxide layer causes the original patterns to increase in width by roughly double the etch depth. To remedy this problem, thinner oxides are required. However, the several hundred eV ion energies in RIE plasmas can lead to significant sputtering of the oxide. To achieve lower ion energies, reactive ion etches based on electron cyclotron resonance (ECR) plasmas have been studied. Using a PlasmaQuest 357 RIE system with ASTeX ECR source, dc biases of less than 10 V have been achieved. Typical Si and GaAs etches consisted of 5 sccm Cl_2 gas flow, 2 mTorr system pressure, 400 W microwave power, and usually no RF power. Fig. 1 shows a structure of OTS on a silicon native oxide (~ 1.5 nm thick) on Si. After a 5 s etch in 6:1 buffered HF, the sample was etched for 60 s in a Cl_2 plasma in the ECR. Although the etch depth here is only ~ 10 nm, the OTS/oxide mask does not show large amounts of damage.

An ideal process would eliminate the wet etch entirely. Fig. 2 shows a structure of ODT on GaAs that was etched with Cl_2 (same parameters as above) without any prior wet processing—after the electron beam exposure, the sample went straight to the ECR. Interestingly, the tone here is negative in the all-dry process. The etch depth (into the unex-

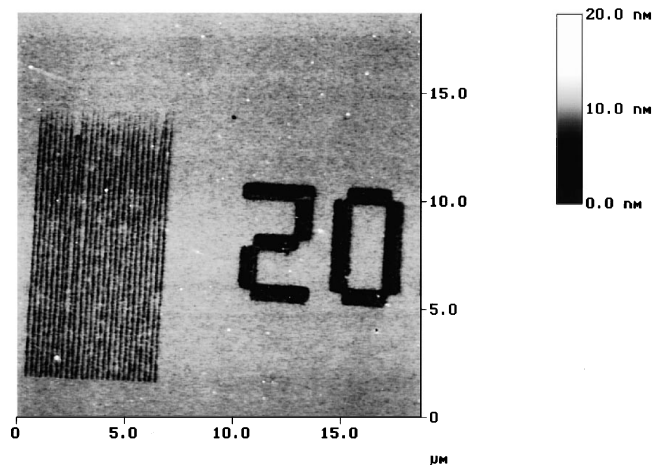


Fig. 1. TMAFM image of a pattern exposed in an OTS layer on a silicon native oxide with a 5 keV electron beam at a dose of $\sim 300 \mu\text{C}/\text{cm}^2$. The pattern was etched into silicon with a low-energy Cl_2 ECR plasma preceded by a very short (5 s) buffered HF etch. Width of lines is ~ 100 nm.

posed region) is ~ 60 nm. This was checked by wet etching a piece from the same ODT/GaAs wafer with a dilute NH_4OH solution, and the wet etch gave a positive tone, see Fig. 3. However, our recent results indicate that it is possible to obtain a positive tone with the ECR based etch of GaAs by using lower electron beam exposure doses and a different etch chemistry. The GaAs was used for these initial dry etch experiments because the native oxide is not as chemically robust as with Si. Initial attempts with SF_6 plasma etching of OTS on Si samples are not conclusive because of the very small etch depths obtained.

IV. ROLE OF BEAM DAMAGE

To examine the change in composition of the monolayer under electron beam irradiation, large areas were exposed with a Perkin Elmer 590 scanning Auger spectrometer at 2 keV beam energy and ~ 500 nA current and a base pressure of $\sim 10^{-10}$ Torr. With these parameters, areas large enough ($\sim 0.25\text{--}1$ cm^2) for further analysis could be easily exposed

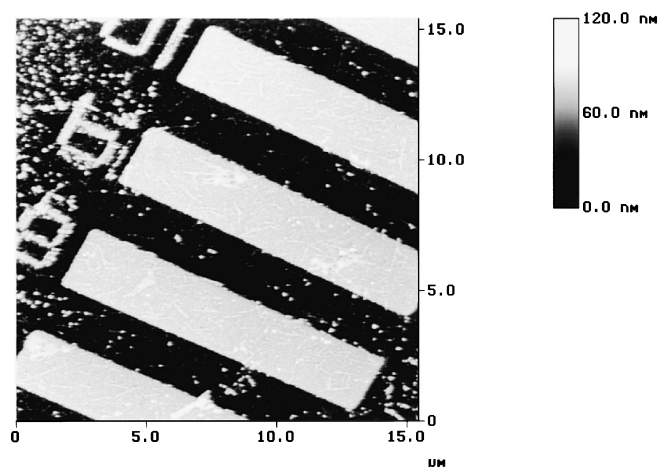


Fig. 2. TMAFM image of a GaAs sample after etching in a Cl_2 ECR plasma using an ODT layer as the resist after patterning at 1 keV. Height of bars is ~ 60 nm.

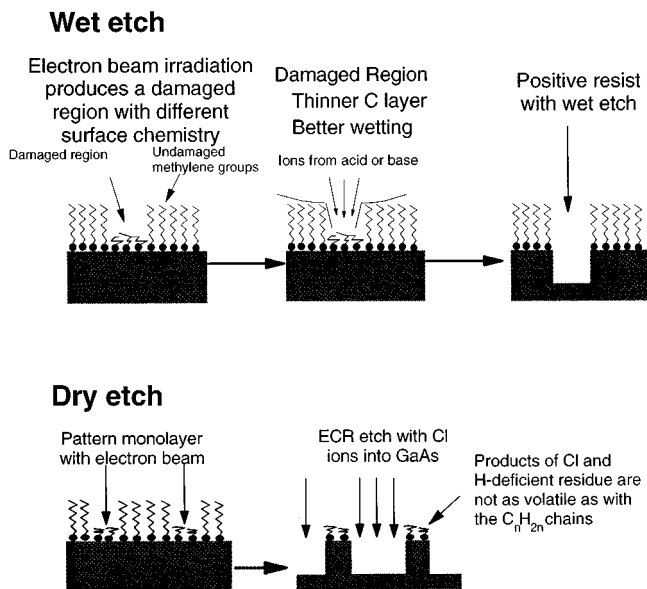


FIG. 3. Schematic of wet and dry etch processes with octadecylthiol layers on GaAs.

in a very clean environment to avoid cracking of contaminants on the surface. The material studied consisted of an OTS layer self-assembled on an evaporated Ti film on GaAs. This differs slightly from the OTS on Si studied by Rieke *et al.*¹⁷ because the Ti substrate allows the study of the role of the Si head-group atom in the monolayer. Auger electron spectroscopy (AES) elemental profiles taken as a function of time (and therefore dose) showed a small decrease in the carbon signal with no noticeable changes in the silicon, oxygen, or titanium signals. However, the large doses that are necessary to produce significant AES signals prevent accurate composition measurements.

The samples that were exposed with the electron beam from the Auger system were transferred to a Surface Science Laboratories SSL-100 x-ray photoelectron spectrometer with monochromatic Al $K\alpha$ source for composition analysis. The samples were transferred through air because the systems are not connected, and this air exposure matches what the samples experience between electron beam exposure and etching. The XPS spectra showed a weak Si($2p$) peak at a binding energy shift of $\sim +2.3$ eV (Ref. 18), which corresponds to Si^{3+} as should be present in the siloxane network at the base of the OTS layer.

The composition was corrected for mean free path differences in the monolayer based on the data of Laibinis *et al.*¹⁹ For these calculations, it was assumed that the siloxane layer ($SiO_{1.5}$) was buried under the carbon chains from the monolayer. The absolute elemental percentage composition depends on the assumed monolayer thickness; however, the same analysis was applied to all samples so that the trends with varying beam dose can be observed.

Because of difficulties in absolute XPS measurements, elemental ratios were compared as a function of electron beam dose. The change in carbon present can be seen by compar-

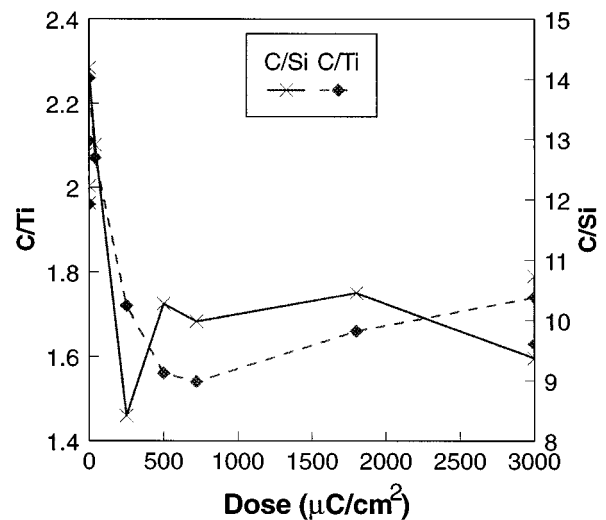


FIG. 4. Carbon to titanium and carbon to silicon ratios from XPS measurements of large areas of an OTS on Ti film after electron beam exposure at 2 keV.

ing the C($1s$) signal to the Ti($2p$) signal from the Ti layer. This C/Ti and C/Si ratios are seen to decrease $\sim 25\%$ – 30% between the zero electron beam dose and doses $500 \mu C/cm^2$ or greater, see Fig. 4, and the Si/Ti ratio is constant. Rieke *et al.* also observed a similar trend in the carbon content.¹⁷ This indicates that the siloxane layer is definitely intact on the surface and that the alkyl component of the monolayer is losing only $\sim 1/4$ of its total carbon content. The carbon decrease is seen to level off at $\sim 500 \mu C/cm^2$, which is a dose that is significantly higher than expected, since the critical dose as measured by AFM and wet etching is $\sim 30 \mu C/cm^2$ (at 1 keV).⁶ After electron beam exposure, the width of the C($1s$) peak increased by ~ 0.1 eV but little shift was observed.

This residual carbon layer cannot result from only atmospheric contamination from the transfer to the XPS system because the Auger data (during the electron beam exposure—with no air exposure) indicates the presence of a large amount of carbon even at very high electron beam doses ($>10 mC/cm^2$). An attempt was made to remove some of the carbon material by treating an electron beam exposed sample ($\sim 1.8 mC/cm^2$) with a solvent rinse immediately before putting it in the XPS system. The overall carbon content was approximately the same as a sample that did not receive the solvent rinsing. This indicates that the carbon residue is not soluble in methylene chloride or ethanol. Interestingly, the C($1s$) spectra of the electron beam exposed, solvent rinsed sample, see Fig. 5, shows a noticeable high binding energy tail that is not present on any of the other samples. The peaks in this tail match binding energies expected for an alcohol group ($-COH$, $+3.3$ eV from $-CH_2-$) and dichloro-carbon group ($-CCl_2$, $+1.58$ eV).²⁰ The unexposed, solvent rinsed sample did not show these solvent retention peaks.

A definite decrease in the contact angle with water is also observed after irradiation. The contact angle decreased from $\sim 115^\circ$ for an unexposed sample to $\sim 60^\circ$ for an OTS on Si sample exposed at $\sim 2 mC/cm^2$. The thicknesses of the dam-

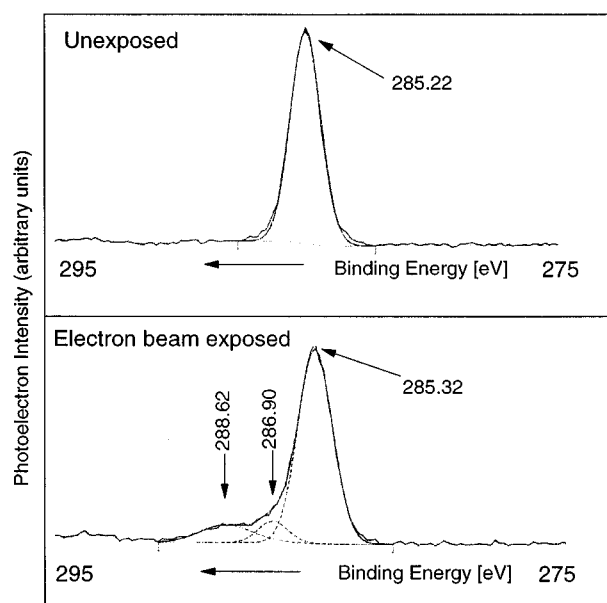


FIG. 5. $C(1s)$ XPS spectra of an electron beam exposed region (bottom) and an unexposed region (top) that were rinsed in methylene chloride and ethanol before introduction into the XPS system (but after electron beam exposure). Peak locations from curve fitting are indicated. The width of the main $C(1s)$ peak is 1.39 eV for the unexposed region and 1.53 eV for the exposed region.

aged films were also checked by ellipsometry. If a fixed index of refraction [$n=1.46$, $k=0$ (Ref. 21)] is assumed, the beam damaged monolayer regions appeared ~ 1 nm thinner than the unexposed regions.

Apparently, a large portion of the carbon from the alkyl chains remains after electron beam exposure. The exact nature of this residue is not known, but since little shift of the carbon peak is observed and the known methylene ($-\text{CH}_2-$) and graphite $C(1s)$ binding energies differ by only ~ 0.1 eV,²⁰ it is likely that the residue consists of cross-linked carbon material.

An interesting parallel can be drawn by comparing data from the radiolysis of hydrocarbons. The density of the alkyl chain ($\rho \sim 0.82$ g/cm³) calculated from the chain number density, composition, and occupied volume in the monolayer is very similar to that of most alkanes.^{3,21} Miller, Lawton, and Balwit²² studied the electron beam irradiation of solid octacosane [$\text{CH}_3(\text{CH}_2)_{26}\text{CH}_3$] and measured yields of various products from hydrogen to octane and the yield of cross-links. Table I shows their yields for octacosane along with a calculation for these yields applied to our monolayers. The deposited beam energy is based on the Bethe stopping power equation²³ calculated for a 2.5 nm carbon layer for a 2 keV electron beam and 500 $\mu\text{C}/\text{cm}^2$ beam dose. The predicted loss of carbon is $\sim 11\%$ and the hydrogen loss is much greater at $\sim 46\%$ so that the starting $\text{C}_{18}\text{H}_{37}$ monolayer would become $\text{C}_{16}\text{H}_{20}$ after the 500 $\mu\text{C}/\text{cm}^2$ beam dose. This could indicate that a similar dehydrogenation is occurring in the monolayer system that leaves behind a residue of cross-linked carbon chains and would be similar to the small decrease in carbon seen in the XPS measurements. Ogawa et al. discovered that after electron beam irradiation of alkyl-

TABLE I. Computed product distribution from the 2 keV electron beam radiolysis at 500 $\mu\text{C}/\text{cm}^2$ of an octacosane layer. The radiolysis yields in column 2 (given in number of products per 100 eV deposited energy) are from the data of Miller, Lawton, and Balwit (Ref. 22). Deposited energy for the electron beam exposure is calculated from the Bethe stopping power (Ref. 23) for a 2.5 nm thick alkane layer. The yield of hydrogen, hydrocarbon products, and cross-links is given both as number per cm² and number per chain. The OTS chain density is assumed to be $\sim 4.5 \times 10^{14}$ chains/cm² (Ref. 21).

Product	G (Number/100 eV)	Number/cm ² $\times 10^{-14}$	Number/chain
H ₂	4.300	270.0	6.01
CH ₄	0.024	1.5	0.03
C ₂ H ₆	0.100	6.3	0.14
C ₄ H ₁₀	0.060	3.8	0.08
C ₅ H ₁₂	0.040	2.5	0.06
C ₆ H ₁₄	0.050	3.1	0.07
C ₇ H ₁₆	0.031	2.0	0.04
C ₈ H ₁₈	0.027	1.7	0.04
Cross-links	2.900	182.0	4.05

siloxanes in He or N₂ atmospheres, the $-\text{CH}_2-$ stretch signal decreased which may be a sign of hydrogen loss and subsequent cross-linking.²⁴

Since some carbon is evidently left behind after monolayer exposure, the positive tone wet etch contrast that is observed must be assisted by a change in surface energy. The unexposed, ordered methylene-terminated regions are known to be very hydrophobic (low surface free energy).²¹ As indicated by wetting, the damaged regions show a higher surface free energy because of compositional or surface arrangement differences that allows for easier etchant penetration through the damaged regions. The surface energy of the unexposed $-\text{CH}_3$ terminated surface has been measured as ~ 21 mJ/m² (Ref. 25), but, in comparison, the energy of a graphite surface is ~ 96 mJ/m² (Ref. 25). These surface free energies roughly correspond to contact angles with water of $\sim 115^\circ$ for the monolayer²¹ and $\sim 50^\circ$ for graphite (calculated from data in Ref. 26). Change in surface free energy and resulting preferential adsorption of materials also have been offered as an explanation for image formation in an SEM for organothiols SAMs on Au.²⁷

The negative resist tone observed in the gas phase etch for GaAs in the ECR ion etching can also be explained since wettability should not play a major role in adsorption. Apparently, the monolayer itself offers very little resistance to the ion etch. Either the Cl^- ions react with the monolayer to produce volatile chlorinated compounds or they diffuse through the monolayer to react with the underlying surface. The carbon residue from the exposure is heavily cross-linked, and may either form a chlorinated polymer by addition of Cl^- ions to the residue (which is not as volatile because the residue is hydrogen deficient) or it may form a better barrier to ion movement to the substrate.

Although the STM exposed surfaces also act as positive resists for wet etching, the exposure process is slightly different in that it takes place in the presence of air (and therefore oxygen). However, a sample of ODT on Au that was exposed with the STM was subsequently inspected with an SEM (at 10 keV beam energy) and then etched in KI/I_2

showed both the STM exposed areas and SEM fields of view.

This information can be used to assist the development of future monolayer processes. Since the alkyl chains are partially cross-linking under irradiation, it is more difficult to form a positive resist from the polymeric material that is left behind. A better positive resist would have a weak bond near the substrate that would easily cleave under irradiation. Alternatively, improving the cross-linking ability would improve the ability of the monolayer to act as a negative resist. The alternative to changing the monolayer is changing the process. There are many possibilities for changing gas chemistry in the low-energy ion etches to achieve more selective etching. A possibility for wet etching that has been mentioned by Rieke *et al.* is removing the carbon residue by a "brief electrochemical oxidation."⁹ However, the addition of chemical oxidants (hydrogen peroxide or nitric acid) to wet etches leads to monolayer breakdown, so it is unclear how this electrochemical oxidation will affect high-resolution patterning and how it will work with insulating substrates. Also, our study has concentrated on subtractive processing, but additive processing through selective metallization has also been demonstrated at high resolution.⁷

V. SUMMARY

High-resolution (<20 nm) patterning has been demonstrated by electron beam lithography of self-assembled monolayers. However, transferring these patterns into the substrate is the more difficult task because of the extreme thinness of the film. Standard wet etches for semiconductors, insulators, and Au have been explored and alkylsiloxanes and alkylthiols act as positive resists with these acid or base etches. Simple multilayer processes have been demonstrated by wet etch transfer of the patterns to a thin mask layer which can subsequently be used for conventional reactive ion etching of the substrate. Dry etches based on ECR plasmas have been used both as a component of the bilayer process and as an all-dry etch of GaAs. In the all-dry Cl₂ etch of GaAs, the monolayer acts as a negative resist. To attempt to explain these tone variations, studies were conducted on electron beam damaged monolayers by composition measurements by XPS. The formation of a carbon residue after exposure plays a major role in the subsequent pattern transfer processes. This information should be of help in determining future monolayers and processes for use of SAMs as high-resolution resists.

ACKNOWLEDGMENTS

The authors would like to acknowledge funding from the Advanced Research Projects Agency in a project monitored

by the Office of Naval Research Grant No. N00014-93-1-1080 and the use of facilities at the Cornell Materials Science Center central facilities funded by the National Science Foundation (NSF) under Award No. DMR-9121654 and facilities at the National Nanofabrication Facility supported by NSF Grant No. ECS-8619049. One author (M.L.) would like to thank the NSF for a Graduate Fellowship, E. Carr for help with XPS measurements, P. Chapman for help in substrate preparation, and P. Simpson for help in substrate etching.

¹L. P. Murray, U. Staufer, E. Bassous, D. P. Kern, and T. H. P. Chang, *J. Vac. Sci. Technol. B* **9**, 2955 (1991).

²A. Ulman, *An Introduction to Ultra-thin Organic Films: Langmuir-Blodgett to Self-Assembly* (Academic, New York, 1991).

³L. H. Dubois, R. G. Nuzzo, *Annu. Rev. Phys. Chem.* **43**, 437 (1992).

⁴R. C. Tiberio, H. G. Craighead, M. Lercel, T. Lau, C. W. Sheen, and D. L. Allara, *Appl. Phys. Lett.* **62**, 476 (1993).

⁵M. J. Lercel, R. C. Tiberio, P. F. Chapman, H. G. Craighead, C. W. Sheen, A. N. Parikh, and D. L. Allara, *J. Vac. Sci. Technol. B* **11**, 2823 (1993).

⁶M. J. Lercel *et al.*, *J. Vac. Sci. Technol. B* **12**, 3663 (1994).

⁷C. R. K. Marrian, F. K. Perkins, S. L. Brandow, T. S. Koloski, E. A. Dobisz, and J. M. Calvert, *Appl. Phys. Lett.* **64**, 390 (1994).

⁸J. A. M. Sondag-Huerthorst, H. R. J. van Helleputte, and L. G. J. Fokkink, *Appl. Phys. Lett.* **64**, 285 (1994).

⁹P. C. Rieke, B. J. Tarasevich, L. L. Wood, M. H. Engelhard, D. R. Baer, G. E. Fryxell, C. M. John, D. A. Laken, and M. C. Jaehnic, *Langmuir* **10**, 619 (1994).

¹⁰G. Gillen, S. Wight, J. Bennett, and M. J. Tarlov, *Appl. Phys. Lett.* **65**, 534 (1994).

¹¹N. Mino, S. Ozaki, K. Ogawa, and M. Hatada, *Thin Solid Films* **243**, 374 (1994).

¹²M. J. Lercel, G. F. Redinbo, H. G. Craighead, C. W. Sheen, and D. L. Allara, *Appl. Phys. Lett.* **65**, 974 (1994).

¹³J. K. Schoer, C. B. Ross, R. M. Crooks, T. S. Corbitt, and M. J. Hampden-Smith, *Langmuir* **10**, 615 (1994).

¹⁴C. B. Ross, L. Sun, and R. M. Crooks, *Langmuir* **9**, 632 (1993).

¹⁵M. Radmacher, R. W. Tillman, M. Fritz, and H. E. Gaub, *Science* **257**, 1900 (1992).

¹⁶P. Chapman and R. Tiberio (unpublished).

¹⁷P. C. Rieke, D. R. Baer, G. E. Fryxell, M. H. Engelhard, and M. S. Porter, *J. Vac. Sci. Technol. A* **11**, 2292 (1993).

¹⁸F. J. Himpsel, F. R. McFeely, A. Taleb-Ibrahimi, and J. A. Yarnoff, *Phys. Rev. B* **38**, 6084 (1988).

¹⁹P. E. Laibinis, C. D. Bain, and G. M. Whitesides, *J. Phys. Chem.* **95**, 7017 (1991).

²⁰C. D. Wagner, W. M. Riggs, and L. E. Davis, *Handbook of X-Ray Photoelectron Spectroscopy*, edited by J. F. Moulder, and G. E. Muilenberg (Perkin-Elmer, Eden Prairie, MN, 1979).

²¹S. R. Wasserman, Yu-T. Tao, G. M. Whitesides, *Langmuir* **5**, 1074 (1989).

²²A. A. Miller, E. J. Lawton, and J. S. Balwit, *J. Phys. Chem.* **60**, 599 (1956).

²³D. C. Joy, and S. Luo, *Scanning* **11**, 176 (1989).

²⁴K. Ogawa, N. Mino, H. Tamura, and M. Hatada, *Langmuir* **6**, 851 (1990).

²⁵N. A. Burnham, D. D. Dominguez, R. L. Mowery, and R. J. Colton, *Phys. Rev. Lett.* **64**, 1931 (1990).

²⁶J. N. Israelachvili, *Intermolecular and Surface Forces* (Academic, London, 1985), pp. 216, 218–220.

²⁷G. P. Lopez, H. A. Biebuyck, and G.M. Whitesides, *Langmuir* **9**, 1513 (1993).